# Radiative weak decays of baryons as single-quark transitions

Frederick J. Gilman and Mark B. Wise
*Stanford Linear Accelerator Center, Stanford University, Stanford, California 94305*
(Received 21 August 1978)

Radiative weak decays are investigated in the context of the quark model assuming the basic transition is an $s$ quark decaying to a $d$ quark plus a photon. This assumption, which encompasses a number of more detailed models, is used to predict relative rates and angular distributions for radiative weak decays of baryons. The measured decay rate for $\Sigma^+ \to p\gamma$ and upper limit on that for $\Xi^- \to \Sigma^-\gamma$ are in disagreement with the predictions and appear to rule out such models.

## I. INTRODUCTION

With the advent of high-energy hyperon beams at Fermilab and the CERN SPS, it will be possible to study even relatively rare hyperon decays in great detail. Among these decays are the radiative weak decays, which are naively expected to occur at the few tenths of a percent level in branching ratio. The decays $\Sigma^+ \to p\gamma$ and $\Xi^0 \to \Lambda\gamma$ are indeed observed at just this level.[1,2,3]

Such weak decays have also been of theoretical interest for some time. Much of the early work[4-7] tended to try to describe the decays in terms of "pole models," where the initial hyperon is changed into an intermediate baryon of increased strangeness by the weak nonleptonic interaction, followed by radiation of a photon, in that order or *vice versa*. While the predicted rate for $\Sigma^+ \to p\gamma$ (the only measured such decay at the time) was more or less of the right order, the corresponding asymmetry parameter was more difficult to predict correctly (although the experimental uncertainties are large).

Such models of the decays have been superceded in recent years by short-distance analyses,[8,9,10] usually within the context of the quark model for hadron structure and for the weak currents. While sometimes disguised in the language of the operator-product expansion, much of the short-distance analysis boils down in the end to finding the local operators which correspond in a particular model to the amplitude for the transition of an $s$ quark to a $d$ quark plus photon. Some diagrams typically included in analyses of this kind for baryon decays are shown in Fig. 1. Other possible diagrams involve Higgs bosons in place of some of all the $W$-boson lines. Without invoking right-handed charged-current couplings of the quarks, such analyses find it difficult to get the asymmetry parameter in $\Sigma^+ \to p\gamma$ to come out correctly.[8,9,10]

In the present paper we do not attempt to explore further particular models of the underlying interactions responsible for radiative weak decays. Instead, we make the rather general assumption that they originate from a strange quark decaying into a down quark with emission of a photon: $s \to d\gamma$ as in Fig. 2. The "black box" for $s \to d\gamma$ includes as a particular case the diagrams in Fig. 1, typical of the short-distance analyses. The most general form of the amplitude for $s \to d\gamma$ is used to calculate relative rates and angular distributions for different hyperon decays.

In the next section we state the theoretical assumptions in more detail and indicate how the parameters of $s \to d\gamma$ at the quark level are reflected at the hadron level. Then in Sec. III predictions for relative decay rates (or equivalently branching ratios) and angular distributions for possible hyperon radiative weak decays are presented. Normalizing to the observed decay $\Sigma^+ \to p\gamma$, the most surprising prediction is that $\Omega^- \to \Xi^-\gamma$ should occur with a rather large branching ratio of several percent. However, we find that the

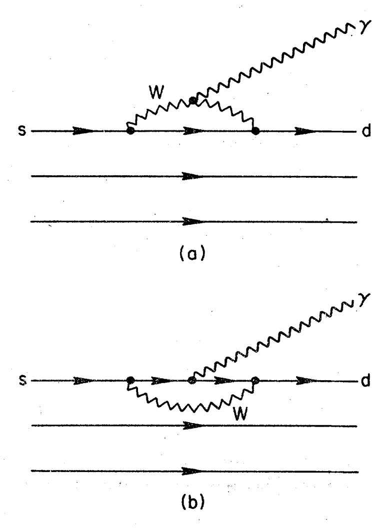


FIG. 1. Some diagrams typically included in short-distance analysis of radiative weak decays of baryons.

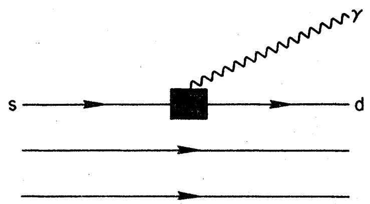


FIG. 2. General diagram for radiative weak baryon decays involving the single-quark transition $s \to d\gamma$.

predicted rate for $\Xi^- \to \Sigma^-\gamma$ is many times larger than the present experimental upper limit. This apparently rules out the general class of models included in the "black box" of Fig. 2. Some comments are stated in Sec. IV.

## II. CONNECTION BETWEEN QUARK AND BARYON RADIATIVE-WEAK-DECAY AMPLITUDES

The decay $s \to d + \gamma$ corresponds to a Feynman amplitude which may be written very generally as[11]

$$\mathfrak{M} = Ge\bar{u}(d)(a + b\gamma_5)i\sigma_{\mu\nu}q_\nu u(s)\epsilon_\mu^{(\gamma)}\,, \tag{1}$$

where $q$ is the four-momentum of the outgoing photon. If quarks were observable as free particles, the amplitude of Eq. (1) would result in the decay width

$$\Gamma(s \to d\gamma) = \frac{G^2e^2}{\pi}(|a|^2 + |b|^2)\,|\vec{q}|^3\,, \tag{2}$$

and an angular distribution relative to the $s$-quark spin of the form

$$1 + \frac{2\,\mathrm{Re}(ab^*)}{|a|^2 + |b|^2}\,\hat{s}\cdot\hat{p}\,,$$

where $\hat{s}$ and $\hat{p}$ are unit vectors along the directions of the spin of the $s$ quark and the three-momentum of the $d$ quark, respectively. The possible presence of both $a$ ("parity-conserving") and $b$ ("parity-violating") amplitudes is a consequence of the parity-violating nature of weak interactions, which must be involved in addition to electromagnetism in order to obtain the decay $s \to d\gamma$.

At the hadron level, one has decays of the form $B_1 \to B_2\gamma$, where $B_1$ and $B_2$ are baryons which differ in strangeness by one unit. It is convenient to describe these decays in terms of helicity coupling constants $g_{\lambda_2\lambda_\gamma}$ labeled by the helicities of the outgoing baryon and photon.[12] The coupling constant $g_{\lambda_2\lambda_\gamma}$ is just the Feynman amplitude in the situation where the initial baryon has spin component $\lambda_1 = \lambda_2 - \lambda_\gamma$ along the direction of the final baryon three-momentum. When $B_1$ has spin component $\lambda_1$ along a given axis (labeled the $z$ axis) the resulting decay angular distribution is

$$\frac{d\Gamma}{d\cos\theta} = \frac{M_2|\vec{q}|}{4\pi M_1}\sum_{\lambda_2,\lambda_\gamma}|g_{\lambda_2\lambda_\gamma}|^2\left|d^{J_1}_{\lambda_1,\lambda_2-\lambda_\gamma}(\theta)\right|^2\,, \tag{3}$$

so that

$$\Gamma(B_1 \to B_2\gamma) = \frac{|\vec{q}|M_2}{2\pi(2J_1+1)M_1}\sum_{\lambda_2,\lambda_\gamma}|g_{\lambda_2\lambda_\gamma}|^2\,, \tag{4}$$

where $\theta$ is the angle between the given axis and the direction of the outgoing baryon.

It is relatively simple now to relate the helicity coupling constant $g_{\lambda_2\lambda_\gamma}$ at the hadron level to the amplitude at the quark level in Eq. (1) if the quark model of hadron structure is employed. In other words we use quark-model SU(6) wave functions for the initial and final baryons and the interaction in Eq. (1) to calculate the matrix elements which correspond to the $g_{\lambda_2\lambda_\gamma}$.

The helicity coupling constants $g_{\lambda_2\lambda_\gamma}$ will then contain several factors: first, a function which depends on the overlap of the initial and final wave functions (as well as the photon momentum), $F(\vec{q})$; second, a spin-dependent factor $C_{\lambda_2\lambda_\gamma}$ which is essentially a Clebsch-Gordan coefficient arising from the quark-spin wave function of the baryons; and third, a factor linear in the amplitudes $a$ and $b$ of Eq. (1).

This last factor is proportional to $Ge|\vec{q}|(a-b)$ when $\lambda_\gamma = +1$ (in which case the initial $s$-quark spin is parallel to the photon three-momentum) and proportional to $Ge|\vec{q}|(a+b)$ when $\lambda_\gamma = -1$ (in which case the initial $s$-quark spin is antiparallel to the photon three-momentum). Therefore we have

$$g_{\lambda_2,+1} = \sqrt{2}\,Ge\,|\vec{q}|(a-b)F(\vec{q})C_{\lambda_2,+1} \tag{5a}$$

and

$$g_{\lambda_2,-1} = \sqrt{2}\,Ge\,|\vec{q}|(a+b)F(\vec{q})C_{\lambda_2,-1}\,. \tag{5b}$$

The spin-dependent factor from the quark-model wave functions of the baryons is the same when all helicities are reversed in sign, i.e., $C_{\lambda_2,+1} = C_{-\lambda_2,-1}$.

The overlap function $F(\vec{q})$ is normalized so that in the nonrelativistic quark model $F(0) = 1$. However, the magnitude of $F(\vec{q})$ is not needed for the calculations in this paper and hence it is not necessary to assume a nonrelativistic regime for the quarks inside baryons. Only relative magnitudes of baryon decay amplitudes will be of interest to us, and they follow solely from the factors $|\vec{q}|C_{\lambda_2\lambda_\gamma}$ provided that (1) $(a \pm b)F(\vec{q})$, as already implicitly assumed, is the same for all initial and final baryons in the quark model ground state;

and (2) $(a\pm b)F(\vec{q})$ varies slowly with $|\vec{q}|$ over the range of photon momentum under consideration. As will be discussed further in Sec. IV, similar assumptions lead to a very successful comparison of theory and experiment when used in the related computation of baryon static and transition magnetic moments and axial-vector coupling constants.

Substituting Eqs. (5) in Eq. (3) and Eq. (4) we find

$$\frac{d\Gamma}{d\cos\theta}=\frac{G^2e^2M_2}{2\pi M_1}|\vec{q}|^3|F(\vec{q})|^2\sum_{\lambda_2}|C_{\lambda_2,+1}|^2\left\{|a-b|^2\left|d^{J_1}_{\lambda_1,\lambda_2-1}(\theta)\right|^2+|a+b|^2\left|d^{J_1}_{\lambda_1,-\lambda_2+1}(\theta)\right|^2\right\} \tag{6}$$

and

$$\Gamma=\frac{2G^2e^2|\vec{q}|^3M_2}{\pi(2J_1+1)M_1}|F(\vec{q})|^2\sum_{\lambda_2}|C_{\lambda_2,+1}|^2(|a|^2+|b|^2). \tag{7}$$

The case where the initial and final baryons have spin $\frac{1}{2}$ is particularly simple. There is only one independent $C_{\lambda_2\lambda_\gamma}$ since $C_{1/2,+1}=C_{-1/2,-1}$, and without loss of generality the initial baryon may be taken as having a spin component $\lambda_1=\frac{1}{2}$ along the $z$ axis (i.e., spin pointing in the $+z$ direction). Equations (6) and (7) then simplify to

$$\begin{aligned}\frac{d\Gamma}{d\cos\theta}&=\frac{G^2e^2M_2}{2\pi M_1}|\vec{q}|^3|F(\vec{q})|^2|C_{1/2,+1}|^2(|a-b|^2\sin^2(\tfrac{1}{2}\theta)+|a+b|^2\cos^2(\tfrac{1}{2}\theta))\\&=\frac{G^2e^2|\vec{q}|^3M_2}{2\pi M_1}|F(\vec{q})|^2|C_{1/2,1}|^2(|a|^2+|b|^2)\left[1+\frac{2\,\mathrm{Re}(ab^*)}{|a|^2+|b|^2}\cos\theta\right]\end{aligned} \tag{8}$$

and

$$\Gamma=\frac{G^2e^2|\vec{q}|^3M_2}{\pi M_1}|F(\vec{q})|^2|C_{1/2,+1}|^2(|a|^2+|b|^2). \tag{9}$$

Aside from some overall factors coming from the baryon wave functions, the expressions for the angular distribution and width at the baryon level, Eqs. (8) and (9), are the same as those at the quark level discussed after Eq. (1). In particular the asymmetry parameter $\alpha=2\,\mathrm{Re}(ab^*)/(|a|^2+|b|^2)$ expressing the correlation between the parent baryon's spin direction and the final baryon's three-momentum, is the same at the quark and baryon level.

## III. PREDICTIONS FOR RADIATIVE WEAK DECAYS OF BARYONS

We are now in a position to calculate the radiative weak decay amplitudes for all baryons in the quark-model ground state for which all the quarks are in a relative $s$ wave. As noted in the last section we assume that the functions $(a\pm b)F(\vec{q})$ are the same for all baryons in the quark-model ground state and that they vary slowly with the photon momentum over the range available in these decays. Thus, in Eq. (7), the main kinematic dependence of the width is the factor of $|\vec{q}|^3$, which reflects the magnetic-dipole nature of all these transitions. The quark-model dynamics enters through the factors $C_{\lambda_2\lambda_\gamma}$.

The predictions for radiative weak decays of baryons in the quark-model ground state[13] are listed in Table I. The column of predicted branching ratios for $B_1\to B_2\gamma$ follows from Eq. (7) using the measured width for $\Sigma^+\to p\gamma$, a factor of $|\vec{q}|^3M_2/[(2J_1+1)M_1]$ from kinematics, the $C_{\lambda_2\lambda_\gamma}$, and the parent-baryon total widths.[14,15]

There is a large disagreement between the predicted rate for $\Xi^-\to\Sigma^-\gamma$ and the experimental upper limit on this decay mode.[3] This alone appears to rule out single-quark transitions, as in Fig. 2, as an explanation of radiative weak decays. In addition, a large branching ratio (~4%) is predicted for $\Omega^-\to\Xi^-\gamma$. This should be readily testable with the high-energy hyperon beams now becoming available and may even be critically tested with data already in hand.[16]

With this in mind, the predictions for angular distributions are of secondary importance, but we state them for completeness. Decays of the form $\frac{1}{2}^+\to\frac{1}{2}^+\gamma$ have an angular distribution $1+\alpha\cos\theta$ where the asymmetry parameter is

$$\alpha=\frac{2\,\mathrm{Re}(ab^*)}{|a|^2+|b|^2}. \tag{10}$$

As noted already in the last section, all such decays then have the same angular distribution as

TABLE I. Predictions for radiative weak baryon decays.

| Decay | $\lvert\vec{q}\rvert$ (MeV) | $C_{\lambda_2,\lambda_\gamma}$ | Predicted branching ratio [a] | Measured branching ratio [b] |
|---|---|---|---|---|
| $\Sigma^+ \to p\gamma$ | 225 | $C_{1/2,1} = +\frac{1}{3}$ | $1.24\times10^{-3}$ (input) | $(1.24\pm0.18)\times10^{-3}$ |
| $\Lambda \to n\gamma$ | 162 | $C_{1/2,1} = \sqrt{6}/2$ | $2.2 \times10^{-2}$ | |
| $\Xi^0 \to \Sigma^0\gamma$ | 117 | $C_{1/2,1} = 5\sqrt{2}/6$ | $9.1 \times10^{-3}$ | $<7 \times10^{-2}$ |
| $\Xi^0 \to \Lambda\gamma$ | 184 | $C_{1/2,1} = -\sqrt{6}/6$ | $4.0 \times10^{-3}$ | $(5\pm5) \times10^{-3}$ |
| $\Xi^- \to \Sigma^-\gamma$ | 118 | $C_{1/2,1} = \frac{5}{3}$ | $1.1 \times10^{-2}$ | $<1.2\times10^{-3}$ |
| $\Omega^- \to \Xi^-\gamma$ | 314 | $C_{1/2,1} = -\sqrt{6}/3$ | $4.1 \times10^{-2}$ | |
| | | $C_{-1/2,1} = \sqrt{2}$ | | |
| $\Omega^- \to \Xi^{*-}\gamma$ | 132 | $C_{3/2,1} = 1$ | $4.5 \times10^{-3}$ | |
| | | $C_{1/2,1} = 2\sqrt{3}/3$ | | |
| | | $C_{-1/2,1} = 1$ | | |

[a] Reference 14.
[b] Particle data group (Ref. 15) and Refs. 1, 2, 3. The branching ratio for $\Xi^0 \to \Lambda^0\gamma$ is given as $(2.3\pm0.7)\times10^{-3}$ in Ref. 2.

the quark decay $s \to d\gamma$. For the decay $\Omega^- \to \Xi^-\gamma$, when the $\Omega^-$ has spin component $\lambda_1$ along the $z$ axis, we have

$$\frac{1}{\Gamma}\frac{d\Gamma}{d\cos\theta} = \tfrac{3}{8}(1+\cos^2\theta + 2\alpha\cos\theta) \tag{11a}$$

when $\lambda_1 = \frac{3}{2}$, and

$$\frac{1}{\Gamma}\frac{d\Gamma}{d\cos\theta} = \tfrac{1}{8}(5 - 3\cos^2\theta + 2\alpha\cos\theta) \tag{11b}$$

when $\lambda_1 = \frac{1}{2}$. The corresponding distributions for $\Omega^- \to \Xi^{*-}\gamma$ are

$$\frac{1}{\Gamma}\frac{d\Gamma}{d\cos\theta} = \tfrac{3}{10}(2 - \cos^2\theta + \alpha\cos\theta) \tag{12a}$$

for $\lambda_1 = \frac{3}{2}$, and

$$\frac{1}{\Gamma}\frac{d\Gamma}{d\cos\theta} = \tfrac{1}{10}(4 + 3\cos^2\theta + \alpha\cos\theta) \tag{12b}$$

when $\lambda_1 = \frac{1}{2}$. The quantity $\alpha$ in Eqs. (11) and (12) is given by Eq. (10). The only measured asymmetry parameter[1] is that for $\Sigma^+ \to p\gamma$ which has the value $-1.03^{+0.52}_{-0.42}$.

## IV. COMMENTS AND CONCLUSION

We have calculated radiative weak baryon decays in the quark model assuming that the basic transition is of the form $s$ quark $\to d$ quark plus photon. Such a single-quark transition encompasses a number of different detailed models which specify the weak interaction dynamics underlying the $s \to d\gamma$ amplitude. In particular, weak-interaction amplitudes corresponding to the diagrams in Fig. 1 are certainly included. Our results, calculated on this basis, for the *relative* radiative weak decay rates of ground-state baryons are in disagreement with experiment. Normalizing to the rate for $\Sigma^+ \to p\gamma$ we predicted a rate for $\Xi^- \to \Sigma^-\gamma$ which is many times larger than the experimental upper limit. In addition, a branching ratio of ~4% is predicted for $\Omega^- \to \Xi^-\gamma$, something which is likely to be ruled out by high-energy hyperon-beam experiments in the near future.

What could be wrong with the theoretical predictions? If we stick with the assumption of a single-quark transition as being responsible for the decays, the other main ingredient of our calculation is that of using the quark model for the initial and final baryons. We consider this unlikely to be at fault in light of the success of closely related calculations of the ratios of baryon axial-vector current couplings (i.e., $F/D$ ratio) and of the baryon magnetic moments, the $\Sigma \to \Lambda\gamma$ transition moment, and the $\Delta^+ \to p\gamma$ transition moment. The successful prediction of the *ratios* of the axial-vector couplings or of all the moments relies on exactly the same assumptions of a single-quark operator transforming like a component of the quark spin and the quark-model wave functions for the baryons involved. Furthermore, the magnitude of the photon momentum $\lvert\vec{q}\rvert$ ranges from zero for the static baryon moments up to ~260 MeV/$c$ for the transition from the $\Delta^+$ to the proton. The agreement of predicted moments[17] to better than 30% argues strongly that the gross disagreement between the experimental and theoretical rates for $\Sigma^+ \to p\gamma$ and $\Xi^- \to \Sigma^-\gamma$ cannot be

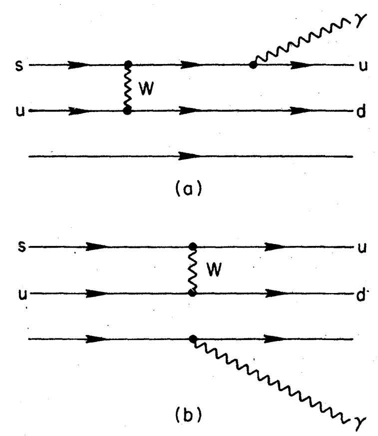


FIG. 3. Some diagrams for radiative weak decays not included in Fig. 2.

explained in this manner.

The other main assumption involved is that only the single-quark transition $s \to d\gamma$ contributes to radiative weak decays. There are in fact other diagrams which could contribute to such decays and which are not included in Fig. 2. Some examples are found in Fig. 3. Diagrams with strong-interaction gluons connecting the quark line(s) inside the $W$-boson loop with the other "spectator" quark lines in Fig. 1 provide another possible example. Presumably it is the presence of these other diagrams which is responsible for the disagreement of the predictions based on single-quark transitions with experiment. Note that the particular diagrams in Fig. 3 cannot contribute to decays such as $\Xi^- \to \Sigma^-\gamma$ or $\Omega^- \to \Xi^-\gamma$. But they can contribute to the amplitude for decays such as $\Sigma^+ \to p\gamma$, interfering constructively or destructively with the amplitude arising from the process in Fig. 2 which has been the main focus of this paper.

The results of this paper indicate that an important part of radiative weak decay amplitudes arises from diagrams other than those included in Fig. 2. Inasmuch as Fig. 2 includes the principal contribution arising from the analysis of the short-distance behavior of the weak currents, these contributions cannot be dominant in all the amplitudes for radiative weak decays. In particular, drawing strong conclusions from comparison of either the overall rate or the asymmetry parameter with the predictions of such analyses would not seem justified.

## ACKNOWLEDGMENTS

This work was supported by the U. S. Department of Energy. One of us (M. B. W.) is also grateful to the National Research Council of Canada and Imperial Oil Ltd. for financial support.

---

[1]L. K. Gershwin *et al.*, Phys. Rev. 188, 2077 (1969).

[2]K. Kleinknecht, in *Proceedings of the XVII International Conference on High Energy Phyics, London, 1974*, edited by J. R. Smith (Rutherford Laboratory, Chilton, Didcot, Berkshire, England, 1974), p. III-23.

[3]N. Yeh *et al.*, Phys. Rev. D 10, 3545 (1974).

[4]R. H. Graham and S. Pakvasa, Phys. Rev. 140, B1144 (1965).

[5]G. Farrar, Phys. Rev. D 4, 212 (1971).

[6]B. Holstein, Nuovo Cimento 2A, 561 (1971).

[7]K. Gavroglu and H.P.W. Gottlieb, Nucl. Phys. B79, 168 (1974).

[8]M. A. Ahmed and G. G. Ross, Phys. Lett. 59B, 293 (1975).

[9]N. Vasanti, Phys. Rev. D 13, 1889 (1976).

[10]M. S. Shifman, A. I. Vainshtein, and V. I. Zakharov, ITEP Report No. ITEP-113, 1976 (unpublished). These authors claim that even with right-handed charged currents one cannot obtain the observed asymmetry parameter for $\Sigma^+ \to p\gamma$.

[11]The Fermi weak coupling constant $G = 1.02 \times 10^{-5}/M_N^2$; $e^2/4\pi \approx \frac{1}{137}$ is the fine-structure constant; $\sigma_{\mu\nu} = (\gamma_\mu\gamma_\nu - \gamma_\nu\gamma_\mu)2i$; and $\epsilon_\mu^{(\gamma)}$ is the polarization vector of the photon. An explicit factor of $Ge$ has been exhibited in the $s \to d\gamma$ amplitude to indicate the order of weak and electromagnetic interactions involved.

[12]The initial (final) baryon, $B_1$ ($B_2$), has spin $J_1$ ($J_2$) and mass $M_1$ ($M_2$). The helicities of the final baryon and photon are $\lambda_2$ and $\lambda_\gamma$, respectively.

[13]The ground-state baryons in the quark model (with $u$, $d$, and $s$ quarks) are the positive-parity SU(3) octet and decuplet. Only baryons with observable weak decays are contained in Table I.

[14]We use the new $\Omega^-$ lifetime value of $(0.82 \pm 0.03) \times 10^{-10}$ sec reported by J. M. Gaillard, invited talk at the Topical Conference of the SLAC Summer Institute on Particle Physics, 1978 (unpublished). All other lifetimes used are from Ref. 15.

[15]Particle Data Group, Phys. Lett. 75B, 1 (1978).

[16]J. M. Gaillard, private communication.

[17]The predictions for baryon moments and their comparison with experiment are reviewed by F. J. Gilman, in *Proceedings of the SLAC Summer Institute on Particle Physics, 1977*, edited by M. C. Zipf, (SLAC, Stanford, 1977), p. 121.